ACS Photonics

Article

pubs.acs.org/journal/apchd5

Spin-Polarized Photon Emission by Resonant Multipolar Nanoantennas

Sergey S. Kruk, Manuel Decker, Isabelle Staude, Stefan Schlecht,† Michael Greppmair,† Dragomir N. Neshev,* and Yuri S. Kivshar

Nonlinear Physics Centre and Centre for Ultrahigh Bandwidth Devices for Optical Systems (CUDOS), Research School of Physics and Engineering, Australian National University, Canberra ACT 0200, Australia

Supporting Information

ABSTRACT: We demonstrate nanoscale spin control of photons emitted by an atomic system coupled to a compact plasmonic nanoantenna supporting phase-locked interference of different multipolar moments within a single resonance. Experimentally we observe *chiral light emission* from quantum dots over split-ring resonant nanoantennas, where the spin of the emitted photons is locked to their transverse momentum. We demonstrate that the polarization can vary from linear to elliptical with ellipticity reaching ±0.5 for emission into opposite halves of the symmetry plane of the nanoantenna.

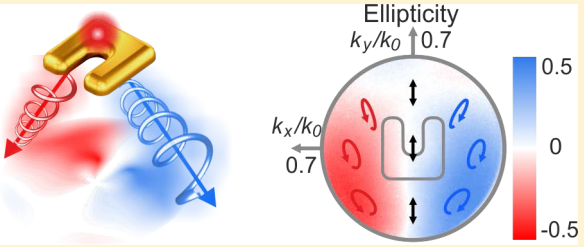

KEYWORDS: *nanoplasmonics, emission control, quantum dots, split-ring resonator, Stokes coefficients*

Light emission from molecular or semiconductor fluorophores is at the foundation of molecular fluorescent spectroscopy and detection of biomolecules and proteins.[1] In recent years, the increased sensitivity of fluorescence spectroscopy techniques has allowed the deterministic detection of molecules with low abundance down to even single-molecule level.[2,3] This has opened a number of important applications, including DNA sequencing,[4] fluorescence nanoscopy of living cells,[5] and molecular labeling.[6] At the heart of fluorescent single-molecule detection is the use of plasmonic nanoantennas, which enable the efficient transfer of the fluorophore emission from the near- to the far-field and vice versa.[7,8] Furthermore, plasmonic nanoantennas enable enhancement of the spontaneous emission rates[9−13] and increased directionality of fluorescent emission,[14] thereby dramatically enhancing the detection efficiency.

Most optical nanoantennas to date draw their functionality from the excitation of electric dipole moments of its constituent elements, hence neglecting higher-order contributions. These contributions, however, become increasingly important for more complex plasmonic nanoparticles supporting strong higher-order multipolar moments,[15−17] thus presenting intriguing opportunities for conceptually new nanoantennas. So far, the research on multipolar plasmonic nanoantennas has focused only on studies of emission enhancement or directivity, including important examples of off-resonant multipolar nanoantennas for directional emission.[18,19]

However, multipolar nanoantennas may also manipulate the polarization state of emission of fluorophores and even control the spin of the emitted photons. Nevertheless, this unique functionality remains largely unexplored to date. Importantly, the emission of photons with different spin by a fluorophore through the use of optical antennas promises a broad range of applications in the control of atomic systems by the photonic environment. Such control can be of interest when selection rules in atomic and molecular transitions have to be obeyed. In particular, the employment of nanoantennas can possibly discriminate between emission of different chiral enantiomers or manipulate the spin of photons emitted by an atom.

Here, we propose and demonstrate the manipulation of the polarization state of light emission in a system of semiconductor quantum dots (QDs) coupled to single-element multipolar nanoantennas. In particular, we show that coupling of QDs to a plasmonic nanoantenna, which is characterized by a superposition of several resonant multipolar contributions (electric/magnetic dipole moments, quadrupole moments, etc.) with a fixed phase difference, leads to the emission of chiral light of opposite handedness from the coupled QD−nanoantenna system. This selective spin-polarized far-field emission from the antenna−emitter system makes our multipolar nanoantenna an ideal candidate for fluorophore detection or advanced light generation. As such, our concept opens a new route to practical nanoscale light sources of spin-polarized photons as well as for simple recognition of emission from chiral emitters of different handedness.

The conventional way for the generation of circularly polarized radiation of different handedness that is well known from radio physics is to employ helical antennas. Transferring this design rule to optics has led to a surge of activities in the field of passive chiral plasmonic structures[20−24] and so-called extrinsically chiral systems.[25−27] Several concepts for chiral light

Received: August 5, 2014
Published: October 14, 2014

generation have been explored. These include the circular emission from QDs coupled to surface plasmons on spiral grooves in metal films,[28,29] as well as selective directional coupling of circularly polarized emitters to metal slot waveguides[30] and hyperbolic media.[31] However, all these examples represent micrometer-sized structures, which contrast with the concept of compact nanoantennas for localized coupling to emitters. Other approaches for generation of circularly polarized radiation are based on phase-retardation techniques;[32] however, they all are highly sensitive to the exact positioning and orientation of the emitter. Altogether, none of the above concepts of chiral light emission allow for reliably controlling the spin of photons (ellipticity and handedness of polarization) emitted from a nanoscale light source.

We overcome these limitations by applying a new approach for circularly polarized light generation based on a multipolar nanoantenna driven in the near-field by an electric dipole emitter, e.g., a QD. Since, in this configuration, the electric and magnetic multipoles of the nanoantenna are normally significantly larger than the dipole moment of the QDs, the far-field emission pattern of the coupled system is dominated by the radiation pattern of the nanoantenna's multipole contributions. Hence, the superposition of the radiation patterns from the dominating multipole contributions of a nanoantenna provides a unique way to generate circularly polarized light. For this purpose, an excitation of at least two multipolar components is required.

We expand the far-field emission of the nanoantenna into a multipolar series and take into account the first three terms of the expansion: the electric dipole moment $\mathbf{p}$, the magnetic dipole moment $\mathbf{m}$, and the electric quadrupole moment $\hat{\mathbf{Q}}$, which at resonance can be written in the form[33]

$$\mathbf{E}(\mathbf{r}) = \frac{k_0^2 e^{i\mathbf{k}_o\mathbf{r}}}{4\pi\varepsilon_0 r}\left([\mathbf{n}\times[\mathbf{p}\times\mathbf{n}]] + \sqrt{\varepsilon_0\varepsilon\mu_0}[\mathbf{m}\times\mathbf{n}] + \frac{ik_o}{6}[\mathbf{n}\times[\mathbf{n}\times\hat{\mathbf{Q}}\mathbf{n}]] + \ldots\right) \quad (1)$$

where $\mathbf{k}_o$ is the photon wavevector, $\mathbf{n} = \mathbf{k}_o/|\mathbf{k}_o|$ is the unit vector in the direction of emission, $\mathbf{r}$ is the coordinate vector, and $r = |\mathbf{r}|$. As the polarization of the field emitted by each multipole is linear, the following requirements need to be fulfilled to obtain circular polarization of the emitted light. First, the electric fields from two multipoles need to be orthogonal to each other. Second, the fields need to have a $\pm\pi/2$ phase difference. Third, the fields need to have the same amplitude. To illustrate how the requirement of orthogonality of fields from the two multipole contributions can be fulfilled, we consider the case where the electric dipole moment $\mathbf{p}$ is oriented along the x-axis, the magnetic dipole $\mathbf{m}$ points in the z direction, and the quadrupole tensor has two nonzero components, $Q_{xy} = Q_{yx}$ (see Figure 1). For this case we can see from the cross products in eq 1 that the electric fields in the x−z plane from the electric dipole $\mathbf{E}_p \propto [\mathbf{n}\times[\mathbf{p}\times\mathbf{n}]]$ is perpendicular to the fields from the magnetic dipole $\mathbf{E}_m \propto [\mathbf{m}\times\mathbf{n}]$ as well as to the electric quadrupole $\mathbf{E}_Q \propto [\mathbf{n}\times[\mathbf{n}\times\hat{\mathbf{Q}}\mathbf{n}]]$. From eq 1 it also follows that a $\pi/2$ phase difference naturally occurs between the electric dipole term $\mathbf{E}_p$ and the electric quadrupole term $\mathbf{E}_Q$ as $\mathbf{E}_Q \propto i = \exp(i\pi/2)$. In addition, we also expect a $\pi/2$ phase difference between $\mathbf{E}_p$ and $\mathbf{E}_m$ for any plasmonic structure that can be described by an LC-circuit model, as for example a U-shaped split-ring resonator (SRR) since, in an LC-circuit picture, the magnetic moment is then given by $\mathbf{m}_{LC} \propto -i\mathbf{p}_{LC}$.[34] Notably, for both cases, we expect the electric-field amplitudes of the superimposed contributing multipole moments to be different in each direction in k-space. This generally leads to the emission of elliptically polarized light with different values of ellipticity for each direction. Due to the orientation and symmetry of the multipole radiation patterns [as reflected in the cross products in eq 1], the polarizations of emission with $k_x < 0$ and $k_x > 0$ have ellipticity with opposite sense of rotation; hence, for emission with $k_x < 0$ and with $k_x > 0$ the photons with opposite spin are dominant. Importantly, the effect of circularly polarized light generation relies on the coherent superposition of multipolar components of a single nanoparticle resonance, which is an inherent property of the resonant antenna and does not require coherence of the excitation process itself.

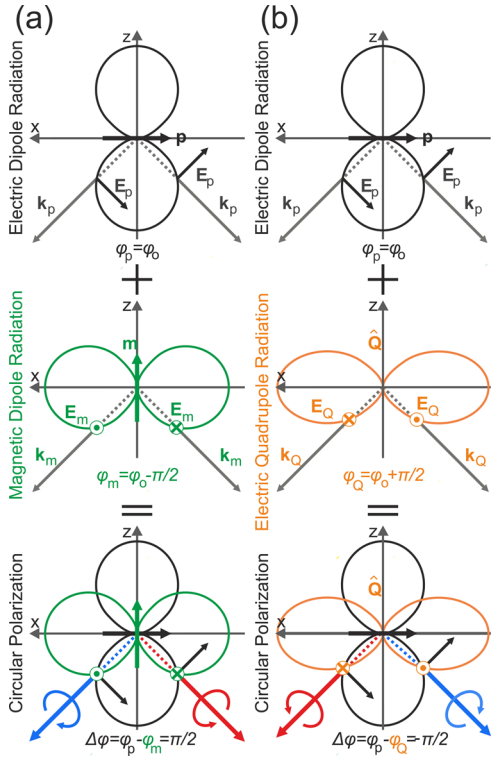

Figure 1. Spin-polarized emission originating from the superposition of (a) the electric field $\mathbf{E}_p$ from an electric dipole $\mathbf{p}$ (black) and the electric field $\mathbf{E}_m$ from a magnetic dipole $\mathbf{m}$ (green) or (b) the electric field $\mathbf{E}_p$ from an electric dipole $\mathbf{p}$ (black) and field $\mathbf{E}_Q$ from an electric quadrupole $\hat{\mathbf{Q}}$ (orange). The maximum electric-field vectors are plotted for different phase factors φ_p, φ_m, and φ_Q relative to a reference phase. The fields fulfill the following requirements: (a) $\mathbf{E}_p \perp \mathbf{E}_m$, $|\mathbf{E}_p| = |\mathbf{E}_m|$, and $\varphi_p - \varphi_m = \pi/2$; (b) similarly $\mathbf{E}_p \perp \mathbf{E}_Q$, $|\mathbf{E}_p| = |\mathbf{E}_Q|$, and $\varphi_p - \varphi_Q = -\pi/2$. Their superposition results in circularly polarized (spin-polarized) emission that is depicted in red (right-handed circular polarization, photon spin +1) and blue (left-handed circular polarization, photon spin −1).

To prove the concept of spin-polarized emission experimentally, we employ SRRs as multipolar nanoantennas coupled to semiconductor QDs emitting at around 800 nm wavelength (see Figure 2). Since SRRs have been a subject of extensive research in the last 10 years,[35−38] their resonant properties and multipolar moments are well understood. On the basis of this knowledge we chose SRRs as a convenient platform for multipolar nanoantenna studies; however, our results remain general and are valid for other types of antennas

dx.doi.org/10.1021/ph500288u | ACS Photonics 2014, 1, 1218−1223

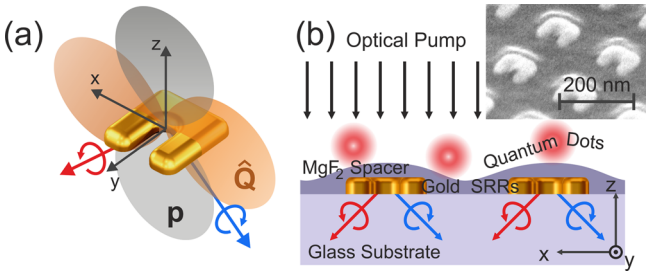

Figure 2. (a) Scheme of an SRR and its radiation pattern at a higher-order resonance consisting of strong electric dipole **p** and electric quadrupole $\hat{\mathbf{Q}}$ (corresponding to Figure 1b). The spin-polarized emission of photons with opposite spins is shown in red (spin +1) and blue (spin −1). (b) Sketch of the studied system. An array of gold SRRs is processed on top of a 1-mm-thick glass substrate via electron-beam lithography and covered with a 12-nm-thick MgF_2 spacer. A layer of randomly distributed QDs is placed on top of the spacer. The system is pumped optically from the top. The inset shows an SEM micrograph of the fabricated SRR array covered with MgF_2 and QDs (not visible).

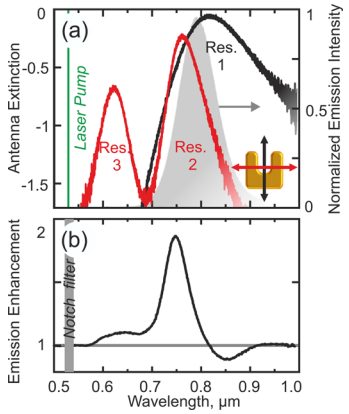

Figure 3. (a) Extinction spectra of the SRR array covered with a MgF_2 spacer layer and a monolayer of QDs for two orthogonal linear polarizations (see inset). The spectra show three resonances at the wavelengths $\lambda_1 \approx 815$ nm, $\lambda_2 \approx 760$ nm, and $\lambda_3 \approx 620$ nm. Each of the resonances is characterized by a unique current distribution (see Supporting Figure S4) that can be connected to its multipolar composition.[16] The gray-shaded region shows the reference spectrum of the QD emission (without SRRs), which is overlapped with resonances 1 and 2. (b) Photoluminescence spectrum of the coupled system of QDs with the SRRs referenced to the PL of the uncoupled QDs on same substrate.

that support multipolar resonances. We fabricate gold SRRs in a periodic lattice with the lattice constant of a = 300 nm on a glass substrate and cover them with a MgF_2 spacer. A uniform layer of QDs is then spin-coated on top of the MgF_2 layer, with a thickness of 12 nm has been chosen to achieve high coupling efficiency between the QDs and the SRRs (Figure 2b). Direct application of the QDs onto the metallic nanostructures could lead to PL quenching, whereas large separation distances would lead to a reduction of the coupling strength. The spin-coating leads to a randomized positioning of the QDs. We therefore investigate how the generation of spin-polarized light is affected by the positioning the emitter in a fixed plane above the SRR. We find that the dominant contribution for spin-polarized emission originates from the emitters positioned close to the center of a SRR (see Figure S5 of the Supporting Information).

To characterize the optical response of the SRRs, first, we collect their extinction spectra $[\ln(1 - T)]$ using a white-light source for excitation. Figure 3a shows the spectra for two orthogonal linear polarizations of the incident plane wave (see inset in Figure 3a). The spectrum is dominated by three resonances (resonances 1−3). For vertical polarization [black line] resonance 1 is excited featuring only a strong electric dipole moment along the y direction. For horizontal polarization [red line] resonances 2 and 3 are excited. These two resonances are often referred to as the SRR higher-order resonances.[13] The fundamental magnetic SRR resonance (not shown) appears at around 1400 nm wavelength and is dominated by an electric dipole moment along the x direction and a magnetic dipole moment along the z direction (see Figure S1 of the Supporting Information), corresponding to the schematic shown in Figure 1a. However, for a typical SRR the scattering cross section of the magnetic dipole is smaller than the scattering cross section of the electric dipole at the fundamental SRR resonance,[16] leading to only a small fraction of the emitted light exhibiting elliptical polarization. Resonance 2, on the other hand, is characterized by a superposition of an electric dipole along the x direction, an electric quadrupole with two nonzero components $Q_{xy} = Q_{yx}$, and a relatively weak magnetic-dipole moment along the z direction,[16] which is neglected in the following. These resonance characteristics correspond to the case shown in Figure 1b. Importantly, for resonance 2 the scattering cross sections of the electric dipole and of the electric quadrupole reach comparable magnitudes,[16] rendering resonance 2 well-suited for the observation of spin-polarized photon emission. Therefore, we focus on this resonance in the following.

To measure the emission of the QD−SRR nanoantenna system, we optically excite the QDs at λ = 532 nm, collect their emission from the substrate side of the sample, and measure the photoluminescence (PL) spectra. Since we use off-resonant pumping of the QDs well below the SRR resonances, the average QD excitation rate is not dependent on the SRR resonances and, hence, independent of the polarization of the pump beam. The QD PL spectrum is shown with gray shading in Figure 3a. Notably, the QD emission overlaps spectrally with the SRR resonances 1 and 2. Figure 3b shows the measured PL signal from the QD−SRR, normalized to the reference PL of the QDs on the plane glass substrate with the MgF_2 layer next to the arrays. Importantly, we observe that even though the SRRs show a pronounced extinction maximum, i.e., a transmission minimum around 800 nm for both polarizations, the emission intensity of the QDs on top of SRRs is approximately a factor of 2 higher than the emission of QDs on the substrate (without SRRs). This enhancement at the resonance wavelengths is a clear signature of coupling between the QDs and the SRRs. Note also that for longer wavelengths at $\lambda \approx 850$ nm, the normalized PL spectrum shows a depletion dip, which is another signature of coupling.[39]

Next, we investigate the polarization properties of the PL signal in Fourier space (k-space), i.e., with regard to different directions of emission. To this end, we perform the same excitation of the QDs and collect the PL signal from the substrate side within the available angle of about 44 degrees that is limited by total internal reflection inside the substrate. After filtering out the excitation signal, we introduce an achromatic quarter-wave plate and a linear polarizer into the optical path to detect a specific polarization state of light. We then record the image of the back-focal plane of the collecting

dx.doi.org/10.1021/ph500288u | ACS Photonics 2014, 1, 1218−1223

objective with a camera (see Figure S6 of the Supporting Information).

The obtained back-focal-plane images allow us to analyze the polarization properties of the emission pattern in k-space via the Stokes parameters formalism in terms of its total intensity I_{tot}, (fractional) degree of polarization ρ, the polarization inclination angle ψ, and the ellipticity $\tan(\chi)$ (see Tables S1 and S2 of the Supporting Information for full set of Stokes parameters and coefficients).

From the Stokes parameters we calculate the polarization state of light for every point of the experimentally accessible part of the k-space and plot the corresponding values for the ellipticity of the resulting polarization state in Figure 4c: an

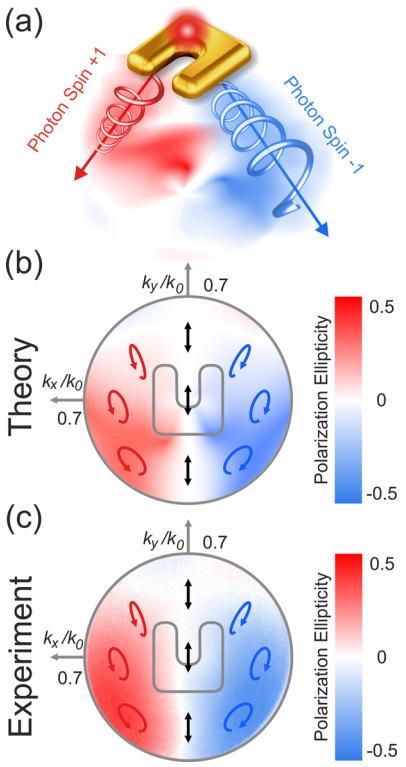

Figure 4. (a) Design concept of a photon spin-polarized emitter. An SRR nanoantenna driven by a quantum dot emits photons with opposite spin in different (opposite) directions. (b) Theoretically calculated and (c) experimentally measured polarization states of emission of the coupled SRR−QD system in different directions (with different k-vectors). The polarization state is encoded in the color as well as in the rotation angle and the elliptical shape of the arrows. The insets in the centers show the corresponding orientation of the SRR.

ellipticity of zero corresponds to linear polarization, while ellipticity values of ±1 correspond to right-handed/left-handed circular polarizations, respectively. Our results show that along the symmetry plane of the SRRs ($k_x = 0$) the emission of the system is vertically polarized and consequently has zero ellipticity, while for $k_x \neq 0$ the emission becomes elliptically polarized. The polarization pattern is mirror-symmetric to the $k_x = 0$ plane. Both the ellipticity and the polarization inclination increase with increasing $|k_x|$. The maximum ellipticity experimentally obtained is ±0.5. For $k_x < 0$ the emission is right-handed elliptically polarized, while for $k_x > 0$ it is left-handed elliptically polarized. Furthermore, we find that the polarization inclination qualitatively follows this behavior, exhibiting opposite inclinations in opposite ($\pm k_x$) semiplanes in k-space. We also observe a non-negligible amount of depolarization in the experiment.

In order to support our experimental results, we perform numerical calculations using CST Microwave Studio. We place a small dipole source over a single SRR on top of a MgF_2 spacer and subsequently extract the polarization state of the emission. We find that the main contribution for the spin-polarized emission of photons can be attributed to QDs that are situated in the center of a single SRR (for details see the Supporting Information). Since in our experiment we average over all orientations of QDs, we calculate the average values for the three cases of the dipole pointing in x-, y-, and z-direction. The results are shown in Figure 4b and well reproduce our experimental measurements of Figure 4c. Our calculations also show that for a single dipole emitter with an optimized orientation and position with respect to the SRR, the emission can be purely circularly polarized in specific directions (see Figure S4d in the Supporting Information). We therefore attribute the experimentally observed depolarization and reduction of the effective overall ellipticity to a maximum value of 0.5 to the incoherent superposition of resonances 1 and 2 of the SRRs, as well as to the random positioning and orientation of QDs.

In conclusion, we have demonstrated that, by using single-element multipolar plasmonic nanoantennas, we can create spin-polarized light emission from a subwavelength light source created by semiconductor QDs coupled to SRRs. We make use of the phase-locked superposition of the radiation fields of the electric dipole and quadrupole contributions of a single SRR resonance to control the direction-dependent polarization state of emission. The polarization state can be further controlled by directional filtering in k-space.

Importantly, the effect of spin-polarized emission is pronounced even for an array of SRRs with randomly distributed QDs. Our novel concept of generating spin-polarized light emission is generally applicable to other types of nanostructures that support multipolar resonances, and it enables the design of compact optical nanoantennas based on single nanoparticles.

Finally, the observed effect of spin-controlled light emission can be linked to the properties of thermal emission of spin-controlled metasurfaces[40] where anisotropic optical antenna patterns result in spin−orbit interaction of light and emission of spin-polarized light with opposite spin in different directions. This emission is considered analogous to the optical spin Hall effect studied recently for passive plasmonic metasurfaces and plasmonic chains.[41,42] As such, our results on spin-controlled light emission with achiral nanoantennas exhibiting two or more multipolar moments open a new efficient route toward spin-controlled photonics with a range of possible applications in molecular detection, quantum light sources, or display technologies.

■ ASSOCIATED CONTENT

Supporting Information

The Supporting Information gives details on the resonances and multipole contributions of the split-ring resonators, as well as on the scenarios of localized dipole excitation. Further details are also provided on the fabrication procedures and the experimental setup for back-focal-plane measurements of the Stokes coefficients. This material is available free of charge via the Internet at http://pubs.acs.org.

dx.doi.org/10.1021/ph500288u | ACS Photonics 2014, 1, 1218−1223

AUTHOR INFORMATION

Corresponding Author

*E-mail: Dragomir.Neshev@anu.edu.au.

Present Address

†S. Schlecht and M. Greppmair: University of Applied Sciences Regensburg, Prüfeninger Strasse 58, 93049 Regensburg, Germany.

Notes

The authors declare no competing financial interest.

ACKNOWLEDGMENTS

We acknowledge the support from the Australian National Fabrication Facility and the Australian Research Council. The authors thank A. Miroshnichenko, A. Evlyukhin, C. Rockstuhl, A. Chipoulin, R. Schiek, and A. F. Koenderink for the useful discussions.

REFERENCES

(1) Lakowicz, J. R. *Principles of Fluorescence Spectroscopy*; Springer: New York, 2007.

(2) Lu, H. P.; Xun, L.; Xie, X. S. Single-molecule enzymatic dynamics. *Science* **1998**, *282*, 1877−1882.

(3) Craighead, H. Future lab-on-a-chip technologies for interrogating individual molecules. *Nature* **2006**, *442*, 387−393.

(4) Eid, J.; Fehr, A.; Gray, J.; Luong, K.; Lyle, J.; Otto, G.; Peluso, P.; Rank, D.; Baybayan, P.; Bettman, B.; Bibillo, A.; Bjornson, K.; Chaudhuri, B.; Christians, F.; Cicero, R.; Clark, S.; Dalal, R.; deWinter, A.; Dixon, J.; Foquet, M.; Gaertner, A.; Hardenbol, P.; Heiner, C.; Hester, K.; Holden, D.; Kearns, G.; Kong, X.; Kuse, R.; Lacroix, Y.; Lin, S.; Lundquist, P.; Ma, C.; Marks, P.; Maxham, M.; Murphy, D.; Park, I.; Pham, T.; Phillips, M.; Roy, J.; Sebra, R.; Shen, G.; Sorenson, J.; Tomaney, A.; Travers, K.; Trulson, M.; Vieceli, J.; Wegener, J.; Wu, D.; Yang, A.; Zaccarin, D.; Zhao, P.; Zhong, F.; Korlach, J.; Turner, S. Real-time DNA sequencing from single polymerase molecules. *Science* **2009**, *323*, 133−138.

(5) Eggeling, C.; Ringemann, C.; Medda, R.; Schwarzmann, G.; Sandhoff, K.; Polyakova, S.; Belov, V. N.; Hein, B.; von Middendorff, C.; Schonle, A.; Hell, S. W. Direct observation of the nanoscale dynamics of membrane lipids in a living cell. *Nature* **2009**, *457*, 1159−1162.

(6) Lu, Y.; Zhao, J.; Zhang, R.; Liu, Y.; Liu, D.; Goldys, E. M.; Yang, X.; Xi, P.; Sunna, A.; Lu, J.; Shi, Y.; Leif, R. C.; Huo, Y.; Shen, J.; Piper, J. A.; Robinson, J. P.; Jin, D. Tunable lifetime multiplexing using luminescent nanocrystals. *Nat. Photonics* **2014**, *8*, 32−36.

(7) Novotny, L.; van Hulst, N. Antennas for light. *Nat. Photonics* **2011**, *5*, 83−90.

(8) Mühlschlegel, P.; Eisler, H.-J.; Martin, O. J. F.; Hecht, B.; Pohl, D. W. Resonant optical antennas. *Science* **2005**, *308*, 1607−1609.

(9) Kühn, S.; Håkanson, U.; Rogobete, L.; Sandoghdar, V. Enhancement of single-molecule fluorescence using a gold nanoparticle as an optical nanoantenna. *Phys. Rev. Lett.* **2006**, *97*, 017402.

(10) Anger, P.; Bharadwaj, P.; Novotny, L. Enhancement and quenching of single-molecule fluorescence. *Phys. Rev. Lett.* **2006**, *96*, 113002.

(11) Aouani, H.; Mahboub, O.; Bonod, N.; Devaux, E.; Popov, E.; Rigneault, H.; Ebbesen, T.; Wenger, J. Bright unidirectional fluorescence emission of molecules in a nanoaperture with plasmonic corrugations. *Nano Lett.* **2011**, *11*, 637−644.

(12) Russell, K. J.; Liu, T.-L.; Cui, S.; Hu, E. L. Large spontaneous emission enhancement in plasmonic nanocavities. *Nat. Photonics* **2012**, *6*, 459−462.

(13) Decker, M.; Staude, I.; Shishkin, I. I.; Samusev, K. B.; Parkinson, P.; Sreenivasan, V. K. A.; Minovich, A.; Miroshnichenko, A. E.; Zvyagin, A.; Jagadish, C.; Neshev, D. N.; Kivshar, Y. S. Dual-channel spontaneous emission of quantum dots in magnetic metamaterials. *Nat. Commun.* **2013**, *4*, 2949.

(14) Curto, A. G.; Volpe, G.; Taminiau, T. H.; Kreuzer, M. P.; Quidant, R.; van Hulst, N. F. Unidirectional emission of a quantum dot coupled to a nanoantenna. *Science* **2010**, *329*, 930−933.

(15) Rockstuhl, C.; Lederer, F.; Etrich, C.; Zentgraf, T.; Kuhl, J.; Giessen, H. On the reinterpretation of resonances in split-ring-resonators at normal incidence. *Opt. Express* **2006**, *14*, 8827−8836.

(16) Mühlig, S.; Menzel, C.; Rockstuhl, C.; Lederer, F. Multipole analysis of meta-atoms. *Metamaterials* **2011**, *5*, 64−73.

(17) von Cube, F.; Irsen, S.; Diehl, R.; Niegemann, J.; Busch, K.; Linden, S. From isolated metaatoms to photonic metamaterials: evolution of the plasmonic near-field. *Nano Lett.* **2013**, *13*, 703−708.

(18) Curto, A. G.; Taminiau, T. H.; Volpe, G.; Kreuzer, M. P.; Quidant, R.; van Hulst, N. F. Multipolar radiation of quantum emitters with nanowire optical antennas. *Nat. Commun.* **2013**, *4*, 1750.

(19) Hancu, I. M.; Curto, A. G.; Castro-López, M.; Kuttge, M.; van Hulst, N. F. Multipolar interference for directed light emission. *Nano Lett.* **2013**, *14*, 166−171.

(20) Decker, M.; Ruther, M.; Kriegler, C. E.; Zhou, J.; Soukoulis, C. M.; Linden, S.; Wegener, M. Strong optical activity from twisted-cross photonic metamaterials. *Opt. Lett.* **2009**, *34*, 2501−2503.

(21) Gansel, J. K.; Thiel, M.; Rill, M. S.; Decker, M.; Bade, K.; Saile, V.; von Freymann, G.; Linden, S.; Wegener, M. Gold helix photonic metamaterial as broadband circular polarizer. *Science* **2009**, *325*, 1513−1515.

(22) Liu, N.; Liu, H.; Zhu, S.; Giessen, H. Stereometamaterials. *Nat. Photonics* **2009**, *3*, 157−162.

(23) Hentschel, M.; Schäferling, M.; Metzger, B.; Giessen, H. Plasmonic diastereomers: adding up chiral centers. *Nano Lett.* **2012**, *13*, 600−606.

(24) Abasahl, B.; Dutta-Gupta, S.; Santschi, C.; Martin, O. J. F. Coupling strength can control the polarization twist of a plasmonic antenna. *Nano Lett.* **2013**, *13*, 4575−4579.

(25) Plum, E.; Liu, X. X.; Fedotov, V. A.; Chen, Y.; Tsai, D. P.; Zheludev, N. I. Metamaterials: optical activity without chirality. *Phys. Rev. Lett.* **2009**, *102*, 113902.

(26) Sersic, I.; van de Haar, M. A.; Arango, F. B.; Koenderink, A. F. Ubiquity of optical activity in planar metamaterial scatterers. *Phys. Rev. Lett.* **2012**, *108*, 223903.

(27) Hendry, E.; Mikhaylovskiy, R. V.; Barron, L. D.; Kadodwala, M.; Davis, T. J. Chiral electromagnetic fields generated by arrays of nanoslits. *Nano Lett.* **2012**, *12*, 3640−3644.

(28) Rui, G.; Chen, W.; Abeysinghe, D. C.; Nelson, R. L.; Zhan, Q. Beaming circularly polarized photons from quantum dots coupled with plasmonic spiral antenna. *Opt. Express* **2012**, *20*, 19297−19304.

(29) Rui, G.; Abeysinghe, D. C.; Nelson, R. L.; Zhan, Q. Demonstration of beam steering via dipole-coupled plasmonic spiral antenna. *Sci. Rep.* **2013**, *3*, 2237.

(30) Rodríguez-Fortuño, F. J.; Marino, G.; Ginzburg, P.; O'Connor, D.; Martínez, A.; Wurtz, G. A.; Zayats, A. V. Near-field interference for the unidirectional excitation of electromagnetic guided modes. *Science* **2013**, *340*, 328−330.

(31) Kapitanova, P. V.; Ginzburg, P.; Rodríguez-Fortuño, F. J.; Filonov, D. S.; Voroshilov, P. M.; Belov, P. A.; Poddubny, A. N.; Kivshar, Y. S.; Wurtz, G. A.; Zayats, A. V. Photonic spin Hall effect in hyperbolic metamaterials for polarization-controlled routing of subwavelength modes. *Nat. Commun.* **2014**, *5*, 3226.

(32) Balanis, C. A. *Antenna Theory - Analysis and Design*, 3rd ed.; John Wiley & Sons, 2005.

(33) Evlyukhin, A. B.; Reinhardt, C.; Chichkov, B. N. Multipole light scattering by nonspherical nanoparticles in the discrete dipole approximation. *Phys. Rev. B* **2011**, *84*, 235429.

(34) Kriegler, C. E.; Rill, M. S.; Linden, S.; Wegener, M. Bianisotropic photonic metamaterials. *IEEE J. Sel. Top. Quant. Electron.* **2010**, *16*, 367−375.

(35) Pendry, J. B.; Holden, A.; Robbins, D.; Stewart, W. Magnetism from conductors and enhanced nonlinear phenomena. *IEEE Trans. Microwave Theory Tech.* **1999**, *47*, 2075−2084.

(36) Linden, S.; Enkrich, C.; Wegener, M.; Zhou, J.; Koschny, T.; Soukoulis, C. M. Magnetic response of metamaterials at 100 terahertz. *Science* **2004**, *306*, 1351−1353.
(37) Decker, M.; Burger, S.; Linden, S.; Wegener, M. Magnetization waves in split-ring-resonator arrays: evidence for retardation effects. *Phys. Rev. B* **2009**, *80*, 193102.
(38) Decker, M.; Feth, N.; Soukoulis, C. M.; Linden, S.; Wegener, M. Retarded long-range interaction in split-ring-resonator square arrays. *Phys. Rev. B* **2011**, *84*, 85416.
(39) Hein, S. M.; Giessen, H. Tailoring magnetic dipole emission with plasmonic split-ring resonators. *Phys. Rev. Lett.* **2013**, *111*, 026803.
(40) Shitrit, N.; Yulevich, I.; Maguid, E.; Ozeri, D.; Veksler, D.; Kleiner, V.; Hasman, E. Spin-optical metamaterial route to spin-controlled photonics. *Science* **2013**, *340*, 724−726.
(41) Yin, X.; Ye, Z.; Rho, J.; Wang, Y.; Zhang, X. Photonic spin Hall effect at metasurfaces. *Science* **2013**, *339*, 1405−1407.
(42) Shitrit, N.; Bretner, I.; Gorodetski, Y.; Kleiner, V.; Hasman, E. Optical spin Hall effects in plasmonic chains. *Nano Lett.* **2011**, *11*, 2038−2042.